ACS APPLIED MATERIALS & INTERFACES

Research Article

www.acsami.org

Simple and Cost-Effective Fabrication of Highly Flexible, Transparent Superhydrophobic Films with Hierarchical Surface Design

Tae-Hyun Kim,[†] Sung-Hun Ha,[†] Nam-Su Jang,[†] Jeonghyo Kim,[‡] Ji Hoon Kim,[†] Jong-Kweon Park,[§] Deug-Woo Lee,[†] Jaebeom Lee,[‡] Soo-Hyung Kim,[†] and Jong-Man Kim*[,†]

[†]Department of Nano Fusion Technology and BK21 Plus Nano Convergence Technology Division, and [‡]Department of Cogno-Mechatronics Engineering, Pusan National University, Busan 609-735, Republic of Korea

[§]Nano Convergence and Manufacturing Systems Research Division, Korea Institute of Machinery and Materials (KIMM), Daejeon 305-343, Republic of Korea

Supporting Information

ABSTRACT: Optical transparency and mechanical flexibility are both of great importance for significantly expanding the applicability of superhydrophobic surfaces. Such features make it possible for functional surfaces to be applied to various glass-based products with different curvatures. In this work, we report on the simple and potentially cost-effective fabrication of highly flexible and transparent superhydrophobic films based on hierarchical surface design. The hierarchical surface morphology was easily fabricated by the simple transfer of a porous alumina membrane to the top surface of UV-imprinted polymeric micropillar arrays and subsequent chemical treatments. Through optimization of the hierarchical surface design, the resultant superhydrophobic films showed superior surface wetting properties (with a static contact angle of >170° and contact angle hysteresis of <3.5°) in the Cassie−Baxter wetting regime, considerable dynamic water repellency (with perfect bouncing of a water droplet dropped from an impact height of 30 mm), and good optical transparency (>82% at 550 nm wavelength). The superhydrophobic films were also experimentally found to be robust without significant degradation in the superhydrophobicity, even under repetitive bending and pressing for up to 2000 cycles. Finally, the practical usability of the proposed superhydorphobic films was clearly demonstrated by examining the antiwetting performance in real time while pouring water on the film and submerging the film in water.

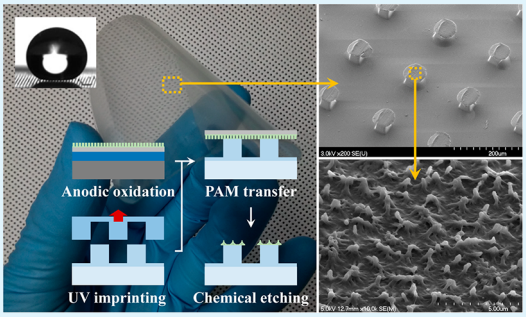

KEYWORDS: *superhydrophobic film, optical transparency, mechanical flexibility, hierarchical surface design, cost-effective fabrication*

1. INTRODUCTION

Over the past decades, superhydrophobic surfaces have attracted great practical interest for various potential applications because of desirable properties such as self-cleaning, water-repelling, antifogging, and anti-icing.[1−5] To date, many attempts have been made to demonstrate nature-inspired functional surfaces with high static contact angle (SCA) and low contact angle hysteresis (CAH) based on various surface geometries and hydrophobic surface modifications.[1−10] In particular, diverse hierarchical surface designs have been introduced as superhydrophobic surface structures, because multiscale geometries are greatly helpful for improving superhydrophobicity.[6−13] In recent years, further research efforts have been made to demonstrate mechanically flexible superhydrophobic films using various fabrication approaches, such as thermally shrinking polymer film,[14] template-assisted polymer replication and subsequent decoration with nanoscale structures,[15,16] polymer replication with hierarchically structured templates,[17,18] lift-up soft-lithography and decoration with nanoparticles,[19] and carbon nanotube (CNT)/polymer coatings.[20] Functional flexible platforms can give superhydrophobic properties to intrinsically hydrophilic materials if they can be easily attached to the surfaces, even with different curvatures.

In addition to superior surface wetting properties and mechanical flexibility, optical transparency of the functional surfaces is also an important performance criterion for expanding application fields to various glass-based products, such as self-cleaning solar panels, antifogging glasses, and raindrop-repellent windows. Some strategies for the fabrication of superhydrophobic films that ensure both flexible and transparent properties have been explored, including polymer replication from templates,[21,22] plasma-based surface texturing,[23,24] laminating exfoliation,[25] sol−gel method,[26] and chemical etching.[27] Nevertheless, functional flexible films with both superior surface wetting properties (SCA of >150° and CAH of <10°) and good optical transparency (transmittance of >80% for visible light) have been rarely reported. This is

Received: December 6, 2014
Accepted: February 17, 2015
Published: February 17, 2015

DOI: 10.1021/am5086066
ACS Appl. Mater. Interfaces 2015, 7, 5289−5295

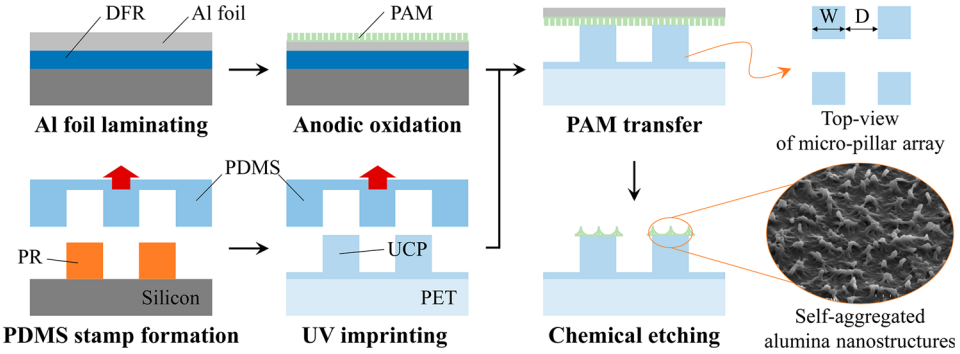

Figure 1. Fabrication process of the hierarchically roughened superhydrophobic films.

probably due to the difficulties in developing efficient methods that can ensure simple, cost-effective, and low-temperature fabrication and overcome the trade-off between the critical performance parameters of superhydrophobicity and optical transparency according to the surface roughness levels.

Anodic oxidation of aluminum (Al) is one of the simplest ways for the fabrication of nanoscale surface structures, such as nanopores and nanopillars. Considerably uniform nanoscale surface morphology can also be easily prepared by self-aggregation of high-aspect-ratio alumina nanowires. Recently, a simple chemical etching of porous alumina membrane (PAM) synthesized by a standard anodic aluminum oxidation (AAO) technique made it possible to easily fabricate self-cleanable plastic films with good superhydrophobicity (SCA of ~164° and CAH of ~5.2°) and moderate transparency (transmittance of ~79% at 550 nm wavelength).[27] Expanding on this development, we introduce a new class of flexible superhydrophobic films with enhanced superhydrophobicity and optical transparency based on a hierarchical surface design. The achievements of this work are that (1) significantly low-cost fabrication can be achieved by using cheap Al cooking foil instead of physical vapor deposition (PVD)-based thin-film Al in an anodization process; (2) hierarchical surface structures can be easily fabricated by transferring the PAM to the top surface of ultraviolet (UV)-imprinted polymeric micropillar arrays and chemically etching the PAM in a controllable manner without a high-temperature process, special fabrication conditions, or expensive vacuum equipment; and (3) both superhydrophobicity and optical transparency of the functional films can be substantially enhanced by simply designing low-density micropillar arrays covered with nanoscale roughness on the top surfaces.

2. EXPERIMENTAL DETAILS

Fabrication of Superhydrophobic Film. The proposed superhydrophobic films based on hierarchical surface design were fabricated by a simple combination of UV imprinting and AAO techniques, as illustrated schematically in Figure 1. The fabrication of the polymeric micropillar arrays started with the formation of an elastomeric stamp based on a standard soft-lithography technique. For this, a ~60-μm-thick photoresist (PR; JSR Micro, THB-151N) mold was first formed on a silicon substrate by a photolithography process. Polydimethylsiloxane (PDMS; Dow Corning, Sylgard 184) prepolymer mixed with a curing promoter at a weight ratio of 10:1 was then poured onto the PR mold, followed by thermal curing at 70 °C for 1 h. After carefully peeling the solidified PDMS from the mold substrate, the preparation of the PDMS stamp with microhole arrays was complete.

For the UV imprinting process, microholes on the PDMS stamp were first filled with a UV-curable polymer (UCP; Norland Products, NOA 61) by manual drop-casting. After the UCP-filled PDMS stamp and polyethylene terephthalate (PET) film were pressed together, the UCP was fully cured by irradiating UV light at an intensity of ~20 mW/cm^2 for 10 min through the transparent PET film. The periodic polymeric micropillar arrays were finally transferred to the PET film by carefully separating the PDMS stamp. In particular, various micropillar arrays were fabricated with different interpillar (edge-to-edge) distances (D) of 30 to 150 μm and a step of 30 μm with respect to the fixed pillar width (W) of 30 μm. These were used to evaluate the surface wetting properties according to variations in surface morphologies (hereafter, surface designs with D/W ratios of 1−5 are denoted as P1−P5, respectively.).

For the AAO process, ~20 μm thick Al cooking foil purchased from a local supermarket was first laminated on a supporting silicon substrate coated with a sacrificial dry film resist (DFR) layer. The sticky surface of the DFR layer was greatly helpful for preventing the foil from physical exfoliation during the subsequent chemical processes. The Al foil was then anodized to form the PAM in a double-jacket beaker containing a solution of 0.3 M oxalic acid ($H_2C_2O_4$) under a constant voltage of 45 V for 15 min. During the anodization process, the solution was constantly maintained at 10 °C using a bath circulator (JEIO TECH, RW-0525G) connected to the beaker.

The PAM was bonded to the polymeric micropillar arrayed film with a thin UCP adhesive that was contact-printed on the pillars' top surface, followed by UV curing with the same irradiation conditions described above. This process results in strong bonding between the PAM and polymeric micropillars. After detaching the supporting silicon substrate by dissolving the sacrificial DFR in acetone, the residual Al was fully etched using an aqueous solution of copper(II) chloride ($CuCl_2$) and hydrochloric acid (HCl) at a temperature of 55 °C. The PAM was then chemically etched using 5 wt % aqueous phosphoric acid (H_3PO_4) solution under a constant temperature of 30 °C.

During the chemical etching of the PAM, the regular nanopores were first revealed and the interpore walls became thinner. With further increases in the etching time, the PAM with nanopores was eventually transformed into high-aspect-ratio nanowires. The free-standing parts of the PAM were entirely removed while leaving nanowire structures anchored firmly on the top surfaces of the micropillars with the intermediate UCP adhesive. The high-aspect-ratio alumina nanowires on the micropillars were finally aggregated at the tips, resulting in the formation of bundles of nanowires (nanoscale roughness), as shown in the inset (SEM) in Figure 1.

Morphological Characterization. The detailed surface morphologies of the fabricated microroughened and hierarchically roughened films were investigated using a field emission scanning electron microscope (FESEM; Hitachi, S4700) and an atomic force microscope (AFM; Park Systems, XE-100).

Contact Angle Measurements. The static and dynamic surface wetting properties of the fabricated films were characterized by measuring the SCA and CAH, respectively. All of the measurements were performed using a contact angle meter (KRÜSS, DSA 20E) equipped with a CCD camera module. The measured values were taken from more than five different regions on each film. Prior to the

DOI: 10.1021/am5086066
ACS Appl. Mater. Interfaces 2015, 7, 5289−5295

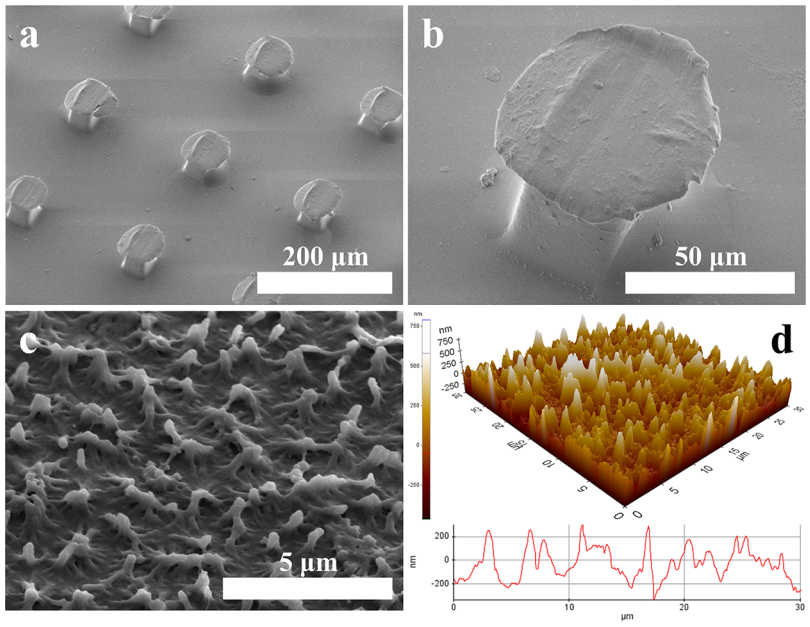

Figure 2. Fabrication results (P4 design) of the hierarchically roughened superhydrophobic film. (a), (b) SEM images of the fabricated film; (c) magnified SEM image and (d) AFM images of nanoscale roughness on top of the micropillars.

measurements, all the fabricated films were hydrophobized by conformally coating a thin fluorocarbon (FC) layer based on a polymerization of octafluorocyclobutane (C_4F_8) in glow discharge. The SCAs of each film were measured with a 7.5 μL deionized (DI) water droplet using a sessile drop method. The dynamic wetting properties were evaluated by analyzing the droplet shapes in real time while sequentially changing the droplet volume using a motorized syringe module built in the contact angle meter. For this, advancing and receding contact angles were first measured with the water droplets growing to 10 μL and shrinking to 5 μL, respectively. The CAHs were then taken from the differences (CAH = advancing CA − receding CA).

Dynamic Water Impact Test. A dynamic water impact test was performed with a 10-μL water droplet dispensed onto the film surfaces from a height of 30 mm. The entire impact process was monitored in real time with a high-speed digital camera (Photron, FASTCAM SA3) capable of recording images at 120 000 frames/s.

Optical Characterization. The optical properties of the fabricated films were evaluated by measuring the transmittance at visible light wavelengths ranging from 400 to 800 nm using UV visible spectroscopy (SCINCO, S310). All transmittances were obtained with respect to air baseline.

Superhydrophobic robustness Test. To characterize the superhydrophobic robustness under mechanical stresses, repetitive bending and pressing deformations for up to 2000 cycles were applied to the film using a motorized mechanical test system (JISC, JSV-H1000) while measuring the SCAs and CAHs every 500 cycles. The cyclic bending test was conducted with a minimum bending radius of 2 mm after firmly clamping both ends of the sample in the test system. One clamp was fixed and the other was moved reversibly to realize repetitive bending and straightening states while precisely controlling the distance between the clamps using the motorized system. The cyclic pressing test was performed under a maximum normal force of 5 N after a covering thin PDMS slab with a thickness of ~1 mm on the sample. The normal force was applied by a flat-top cylindrical metallic rod after making an intimate contact between the sample and rod and precisely specified with a push−pull force gauge (JISC, H-10) equipped in the test system. The measurements of SCAs and CAHs were performed on at least five different regions including the stressed areas in the unloaded states.

Practical Anti-Wetting Test. A practical antiwetting test was conducted by observing the fabricated superhydrophobic film attached to a slide glass in real time while pouring DI water on the film and submerging the film in DI water.

3. RESULTS AND DISCUSSION

Figure 2a, b shows the SEM images of the hierarchically roughened surface made of arrayed polymeric micropillars (microscale roughness) with self-aggregated alumina nanowires (nanoscale roughness) on the top surface. Clearly, the surface morphology was stably created while maintaining the geometrical periodicity even after transferring the nanoscale protruding features thanks to the well-ordered micropillar arrays. The nanoscale roughness on top of the micropillar was more precisely observed through the SEM and AFM investigations, as shown in Figure 2c, d, respectively. The SEM and AFM images indicate that the nanoscale protrusions made of the aggregated nanowires were produced with quite uniform spatial distribution, though relatively low-quality Al foil was used in the anodization process. This means that morphological uniformity of the resulting nanoscale roughness is relatively independent with the regularity of nanopores on the PAM, resulting in reproducible fabrication. The results suggest that the simple and cost-effective fabrication approach is useful for demonstrating flexible and transparent functional films with hierarchical surface design. More importantly, the process can potentially be scaled up for large-area fabrication, as demonstrated in Figure S1 in the Supporting Information.

Figure 3 shows the SCAs and CAHs measured on the microroughened and hierarchically roughened films. The SCA of the PET film coated with polymer (P0 design) was 117.7 ± 0.5° after the hydrophobic FC coating. The static wetting property of the film was modified by designing micropillar arrays, as shown in Figure 3a. The SCA of the microroughened film was gradually increased when increasing the D/W ratio up to 4 (P4 design; 157.8 ± 0.5°) while satisfying the Cassie−Baxter wetting criteria, as shown in Figure S2 in the Supporting Information. However, the SCA suddenly decreased to 113.7 ± 0.9° when the interpillar distance reached 5 (P5 design). In this case, the water droplet fully penetrated into the space between

DOI: 10.1021/am5086066
ACS Appl. Mater. Interfaces 2015, 7, 5289−5295

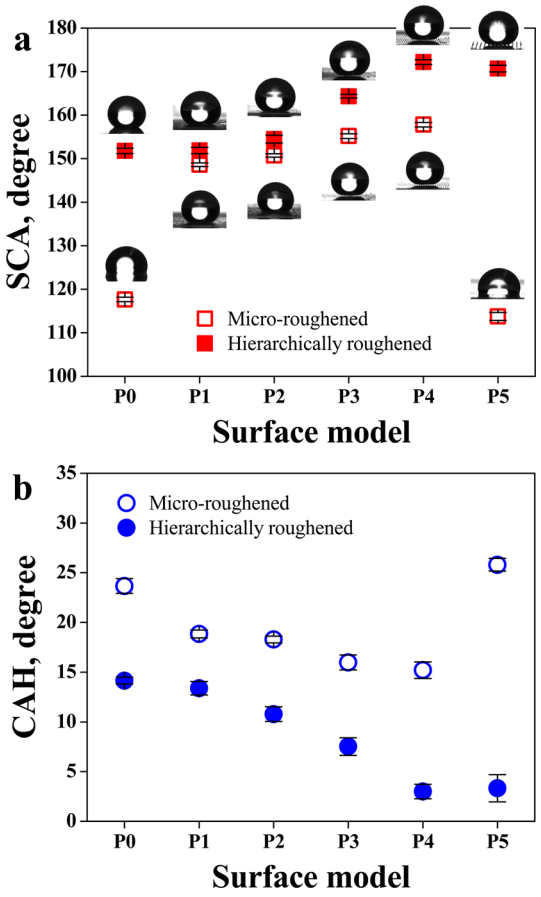

Figure 3. Surface wetting properties of microroughened and hierarchically roughened films. (a) static contact angle (insets: digital images of water droplets sitting on each film), and (b) contact angle hysteresis.

the micropillars, as shown in the digital image of water droplet sitting on the microroughened P5 film in the inset of Figure 3a. This means that the wetting state of the microroughened film is changed to the Wenzel wetting mode, mainly due to the interpillar distance that was sufficiently large to cause a transition from a composite solid–air–liquid interface to a solid–liquid interface.

After transferring the nanoscale roughness to the PET film, the SCA was significantly increased to 151.8 ± 0.6°, which originates from the formation of a composite interface with many air-pockets. In agreement with the Cassie–Baxter wetting model, the SCA of the hierarchically roughened film was also gradually increased with increasing D/W ratio, revealing much higher values compared to those of each microroughened counterpart, as shown in Figure 3a. Interestingly, no transition to the Wenzel state was found on the hierarchically roughened P5 film in contrast to the same surface design with a microroughened film. These experimental observations clearly suggest that the proposed hierarchical surface design is useful for efficiently reducing the solid-fraction and forming a composite interface with sufficient air-pocket sites, resulting in considerable improvement of the static wetting properties.

Figure 3b shows the CAHs characterized on the fabricated functional films. The CAHs of both the microroughened and hierarchically roughened films were gradually decreased with increasing D/W ratio up to 4 (P4 design), which is mainly attributed to the reduction of the actual contact area between the water droplet and film surface due to the roughness effect. However, more remarkable enhancement of the dynamic wetting properties was found on the hierarchically roughened films, because the actual contact area can be further reduced with the formation of the nanoscale roughness on top of the micropillars. In addition, a sharp increase of the CAH was observed on the microroughened P5 film, whereas the hierarchically roughened film with the same surface design still maintained a low CAH of less than 3.5°, as shown in Figure 3b. This clearly suggests that the proposed hierarchical surface design plays a key role in ensuring the superior superhydrophobicity and superhydrophobic robustness in the Cassie–Baxter regime.

The water-repellence of the microroughened and hierarchically roughened P4 films was investigated by a dynamic water impact test. Figure 4 shows the sequential digital images of a water droplet taken every 4 ms during the test. The water droplet impinging on the microroughened film did not bounce from the surface, as shown in Figure 4a. It eventually stuck to the surface while fully wetting the surface structures after fluctuating slightly. This implies that the water hammer pressure exceeds the antiwetting capillary pressure of the film. In contrast, the water droplet was entirely repelled from the hierarchically roughened film within 20 ms after impinging without any satellite droplets remaining on the surface, as shown in Figure 4b. This means that the nanoscale roughness on top of the micropillars is crucial for amplifying the antiwetting pressure that makes the superhydrophobic behavior of the film quite robust even under dynamic conditions.

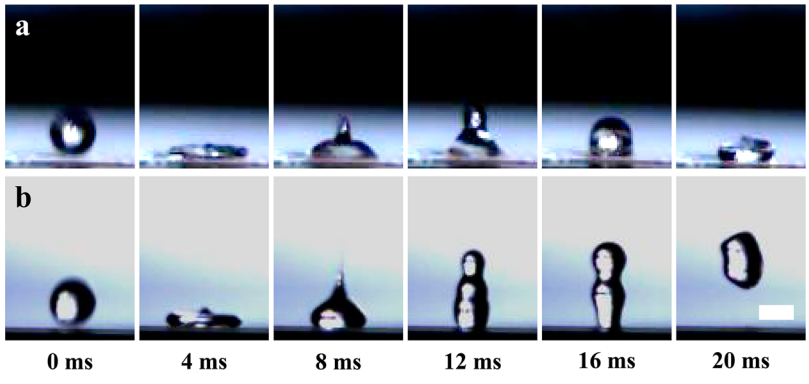

Figure 4. Dynamic water impact test on (a) microroughened and (b) hierarchically roughened films (P4 design) from a drop height of 30 mm (scale bar: 2 mm).

DOI: 10.1021/am5086066
ACS Appl. Mater. Interfaces 2015, 7, 5289–5295

Figure 5 shows the transmittance values examined on the microroughened and hierarchically roughened films at a wavelength of 550 nm. The full transmittance curves of the films at visible light wavelengths (400 to 800 nm) are shown in Figure S3 in Supporting Information. The transmittance of the intrinsic film (PET film coated with polymer) was ~92.6% at 550 nm, which decreased after making the surfaces rough. A steep degradation in optical transparency was found on the P1 films mainly due to the scattering effect from the rough surfaces, but the films gradually became transparent with increasing interpillar distance, as shown in Figure 5.

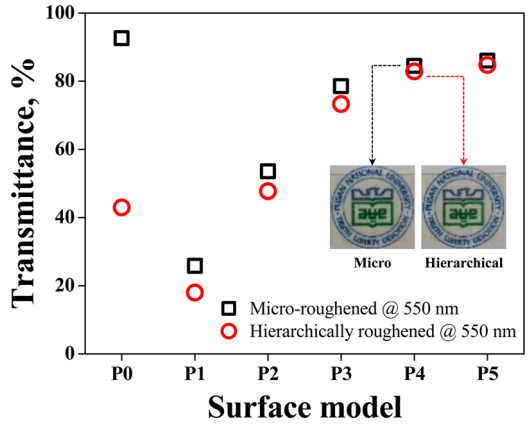

Figure 5. Optical properties of microroughened and hierarchically roughened films examined at a wavelength of 550 nm (insets: digital images of each film (P4 design) placed on the papers with a logo of our institution).

The transmittance values measured on the microroughened films were higher than those on the hierarchically roughened ones for all the surface designs. This probably originates from the nanoscale roughness (P0 design; ~42.9% at 550 nm) on top of the micropillars further hindering the transmission of incoming light through the hierarchically roughened films. However, the degradation in the optical properties of the hierarchically roughened films compared to the microroughened films was gradually alleviated with increasing interpillar distance, as shown in Figure 5 and Figure S4 in the Supporting Information.

The transmittance values of the hierarchically roughened P4 and P5 films were higher than 82% with a minimal degradation of less than 2% compared to the microroughened films with the same designs. This was also verified by the fact that the logo of our institution could be clearly seen through each film without appreciable differences between the microroughened and hierarchically roughened P4 films, as shown in the insets of Figure 5. This is mainly due to the decrease of the translucent portion (with nanoscale roughness) on the hierarchically roughened film with the sparser micropillars. This clearly indicates that the proposed hierarchical surface design makes it possible to efficiently demonstrate functional films that ensure superior superhydrophobicity and optical transparency at the same time.

The superhydrophobic robustness of the hierarchically roughened superhydrophobic films (P4 design) under mechanical stresses was investigated by repetitive bending and pressing tests for up to 2000 cycles. Figure 6a, b shows the SCAs and CAHs of the film measured every 500 cycles during the bending and pressing tests, respectively. The surface wetting properties of the films were retained without appreciable degradation compared to the initial values even after finishing the tests, as shown in Figure 6. In addition to the superior superhydrophobicity and optical transparency, the superhydrophobic robustness of the films is also of great importance for expanding the applicability of the functional films to even glass-based products with different curvatures, as demonstrated in Figure S5 in the Supporting Information.

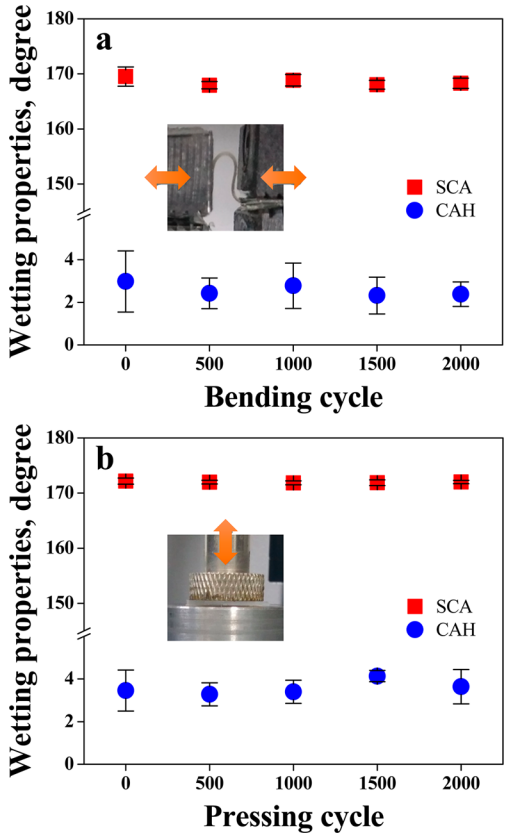

Figure 6. Superhydrophobic robustness of hierarchically roughened superhydrophobic films (P4 design). Changes in surface wetting properties due to (a) repetitive bending tests with a minimum bending radius of 2 mm (with respect to initial SCA of 169.5 ± 1.7° and CAH of 3 ± 1.4°) and (b) repetitive pressing tests with a maximum normal force of 5 N (with respect to initial SCA of 172.2 ± 0.5° and CAH of 3.5 ± 1°).

The usability of the proposed superhydrophobic films was practically examined by simple antiwetting tests. Figure 7 shows digital images of the superhydrophobic films attached to a slide glass for the tests. The DI water easily bounced off the film immediately after being poured onto it, clearly indicating good water-repellency, as shown in Figure 7a. In addition, it was also found that the film did not become wet even after being submerged in DI water, as shown in Figure 7b. The test results in Figure 7a, b also revealed that some portions of the DI water remained on the surface of the slide glass without covering the superhydrophobic film after the tests. The red arrows in Figure 7a, b indicate some DI water portions remaining on the surface. The experimental observations clearly suggest that the proposed films can be easily employed as antiwetting surfaces in glass-based applications because of their superior surface wetting properties, good optical transparency, and mechanical flexibility.

DOI: 10.1021/am5086066
ACS Appl. Mater. Interfaces 2015, 7, 5289−5295

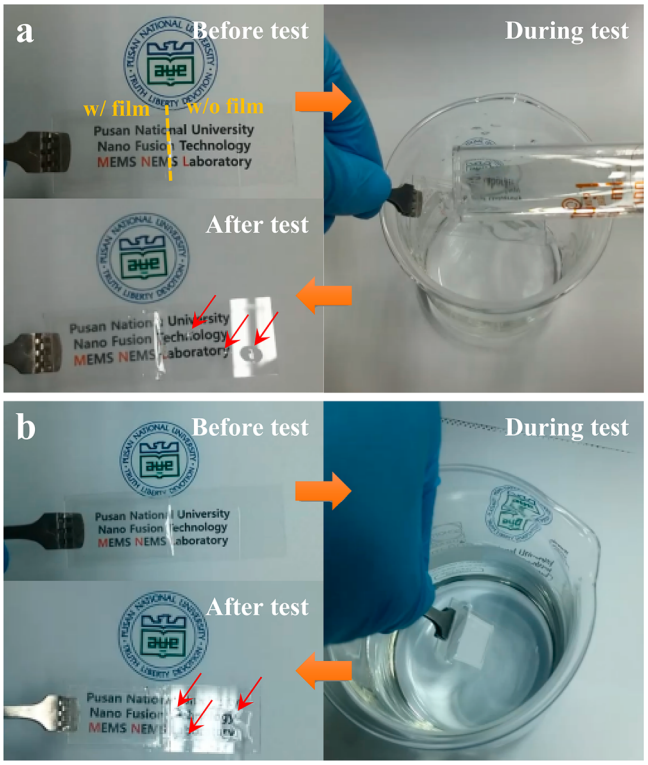

Figure 7. Practical antiwetting tests with the fabricated superhydrophobic film (P4 design). Digital images of the film attached to a slide glass before, during and after (a) pouring the DI water on the film, and (b) submerging the film in the DI water (the red arrows indicate some DI water portions remaining on the surface without covering the superhydrophobic film after the tests).

4. CONCLUSION

A simple and cost-effective fabrication method was proposed for high-performance hierarchical superhydrophobic films that ensure both optical transparency and mechanical flexibility. The dual-scale functional surface textures were simply fabricated by transferring PAM to the top surface of UV-imprinted polymeric micropillar arrays with a polymer adhesive and chemically treating the transferred PAM. With the hierarchical surface design, superior superhydrophobicity with SCA higher than 170° and CAH less than 3.5° was demonstrated on the highly flexible plastic films, along with optical transparency higher than 82% at a wavelength of 550 nm and good water-repellency. In addition, the surface wetting properties of the superhydrophobic film were stably retained without significant degradation even after 2000 cycles of repetitive bending with a minimum bending radius of 2 mm and pressing under a maximum normal force of 5 N. The antiwetting tests clearly confirmed that the proposed superhydrophobic films could have a variety of practical applications, even with various glass-based products.

■ ASSOCIATED CONTENT

Supporting Information

Digital images of large-area (4 in. wafer-scale) superhydrophobic surface fabricated on PET and glass substrates (Figure S1), theoretical estimation of static wetting properties of the microroughened film according to variations in D/W ratio with the Wenzel and Cassie–Baxter models (Figure S2), transmittance curves measured on microroughened and hierarchically roughened films at a wavelength ranging from 400 to 800 nm (Figure S3), percent degradation in optical transmittances at 550 nm wavelength of hierarchically roughened films with respect to those of microroughened counterparts (Figure S4), digital images of the superhydrophobic films attached to glass-based products with different curvatures (Figure S5). This material is available free of charge via the Internet at http://pubs.acs.org.

■ AUTHOR INFORMATION

Corresponding Author

*E-mail: jongkim@pusan.ac.kr.

Notes

The authors declare no competing financial interest.

■ ACKNOWLEDGMENTS

This work was supported by "Development of Next Generation Multi-functional Machining Systems for Eco/Bio Components" project of Ministry of Knowledge Economy and the Civil & Military Technology Cooperation Program through the National Research Foundation of Korea (NRF) funded by the Ministry of Science, ICT & Future Planning (2013M3C1A9055407).

■ REFERENCES

(1) Yao, X.; Song, Y.; Jiang, L. Application of Bio-Inspired Special Wettable Surfaces. *Adv. Mater.* **2012**, *23*, 719–734.
(2) Xue, C.-X.; Jia, S.-T.; Zhang, J.; Ma, J.-Z. Large-Area Fabrication of Superhydrophobic Surfaces for Practical Applications: An Overview. *Sci. Technol. Adv. Mater.* **2010**, *11*, 033002.
(3) Nosonovsky, M.; Bhushan, B. Superhydrophobic Surfaces and Emerging Applications: Non-Adhesion, Energy, Green Engineering. *Curr. Opin. Colloid Interface Sci.* **2009**, *14*, 270–280.
(4) Li, X.-M.; Reinhoudt, D.; Crego-Calama, M. What Do We Need for Superhydrophobic Surface? A Review on the Recent Progress in the Preparation of Superhydrophobic Surfaces. *Chem. Soc. Rev.* **2007**, *6*, 1350–1368.
(5) Zhang, Y.-L.; Xia, H.; Kim, E.; Sun, H.-B. Recent Developments in Superhydrophobic Surfaces with Unique Structural and Functional Properties. *Soft Matter* **2012**, *8*, 11217–11231.
(6) Hsu, S.-H.; Woan, K.; Sigmund, W. Biologically Inspired Hairy Structures for Superhydrophobicity. *Mater. Sci. Eng., R* **2011**, *72*, 189–201.
(7) Yan, Y. Y.; Gao, N.; Barthlott, W. Mimicking Natural Superhydrophobic Surfaces and Grasping the Wetting Process: A review on Recent Progress in Preparing Superhydrophobic Surfaces. *Adv. Colloid Interface Sci.* **2011**, *169*, 80–105.
(8) Roach, P.; Shirtcliffe, N. J.; Newton, M. I. Progress in Superhydrophobic Surface Development. *Soft Matter* **2008**, *4*, 224–240.
(9) Celia, E.; Darmanin, T.; Givenchy, E. T.; Amigoni, S.; Guittard, F. Recent Advances in Designing Superhydrophobic Surfaces. *J. Colloid Interface Sci.* **2013**, *402*, 1–18.
(10) Liu, K.; Tian, Y.; Jiang, L. Bio-Inspired Superhydrophobic and Smart Materials: Design, Fabrication, and Application. *Prog. Mater. Sci.* **2013**, *58*, 503–564.
(11) Gao, L.; McCarthy, T. J. The "Lotus Effect" Explained: Two Reasons Why Two Length Scales of Topography Are Important. *Langmuir* **2006**, *22*, 2966–2967.
(12) Nosonovsky, M.; Bhushan, B. Hierarchical Roughness Makes Superhydrophobic States Stable. *Microelectron. Eng.* **2007**, *84*, 382–386.
(13) Sahoo, B. N.; Kandasubramanian, B. Recent Progress in Fabrication and Characterisation of Hierarchical Biomimetic Superhydrophobic Structures. *RSC Adv.* **2014**, *4*, 22053.
(14) Manna, U.; Carter, M. C. D.; Lynn, D. M. "Shrink-to-Fit" Superhydrophobicity: Thermally-Induced Microscale Wrinkling of

DOI: 10.1021/am5086066
ACS Appl. Mater. Interfaces 2015, 7, 5289–5295

Thin Hydrophobic Multilayers Fabricated on Flexible Shrink-Wrap Substrates. *Adv. Mater.* **2013**, *25*, 3085−3089.
(15) Xu, M.; Lu, N.; Xu, H.; Qi, D.; Wang, Y.; Shi, S.; Chi, L. Fabrication of Flexible Superhydrophobic Biomimic Surfaces. *Soft Matter* **2010**, *6*, 1438−1443.
(16) Ko, H.; Zhang, Z.; Takei, K.; Javey, A. Hierarchical Polymer Micropillar Arrays Decorated with ZnO Nanowires. *Nanotechnology* **2010**, *21*, 295305.
(17) Lee, Y.; Park, S.-H.; Kim, K.-B.; Lee, J.-K. Fabrication of Hierarchical Structures on a Polymer Surface to Mimic Natural Superhydrophobic Surfaces. *Adv. Mater.* **2007**, *19*, 2330−2335.
(18) Xu, M.; Lu, N.; Qi, D.; Xu, H.; Wang, Y.; Shi, S.; Chi, L. Fabrication of Superhydrophobic Polymer Films with Hierarchical Silver Microbowl Array Structures. *J. Colloid Interface Sci.* **2011**, *360*, 300−304.
(19) Yao, T.; Wang, C.; Lin, Q.; Li, X.; Chen, X.; Wu, J.; Zhang, J.; Yu, K.; Yang, B. Fabrication of Flexible Superhydrophobic Films by Lift-Up Soft-Lithography and Decoration with Ag Nanoparticles. *Nanotechnology* **2009**, *20*, 065304.
(20) Wang, C.-F.; Chen, W.-Y.; Cheng, H.-Z.; Fu, S.-L. Pressure-Proof Superhydrophobic Films From Flexible Carbon Nanotube/Polymer Coatings. *J. Phys. Chem. C* **2010**, *114*, 15607−15611.
(21) Kim, M.; Kim, K.; Lee, N. Y.; Shin, K.; Kim, Y. S. A Simple Fabrication Route to a Highly Transparent Super-Hydrophobic Surface with a Poly(dimethylsiloxane) Coated Flexible Mold. *Chem. Commun.* **2007**, *22*, 2237−2239.
(22) Im, M.; Im, H.; Lee, J.-H.; Yoon, J.-B.; Choi, Y.-K. A Robust Superhydrophobic and Superoleophobic Surface with Inverse-Trapezoidal Microstructures on a Large Transparent Flexible Substrate. *Soft Matter* **2010**, *6*, 1401−1404.
(23) Tserepi, A. D.; Vlachopoulou, M.-E.; Gogolides, E. Nano-texturing of Poly(dimethylsiloxane) in Plasmas for Creating Robust Super-Hydrophobic Surfaces. *Nanotechnology* **2006**, *17*, 3977−3983.
(24) Mundo, R. D.; Palumbo, F.; d'Agostino, R. Nanotexturing of Polystyrene Surface in Fluorocarbon Plasmas: From Sticky to Slippery Superhydrophobicity. *Langmuir* **2008**, *24*, 5044−5051.
(25) Zhang, Z.-X.; Li, Y.; Ye, M.; Boonkerd, K.; Xin, Z.; Vollmer, D.; Kim, J. K.; Deng, X. Fabrication of Superhydrophobic Surface by a Laminating Exfoliation Method. *J. Mater. Chem. A* **2014**, *2*, 1268−1271.
(26) Budunoglu, H.; Yildirim, A.; Guler, M. O.; Bayindir, M. Highly Transparent, Flexible, and Thermally Stable Superhydrophobic ORMOSIL Aerogel Thin Films. *ACS Appl. Mater. Interfaces* **2011**, *3*, 539−545.
(27) Kong, J.-H.; Kim, T.-H.; Kim, J. H.; Park, J.-K.; Lee, D.-W.; Kim, S.-H.; Kim, J.-M. Highly Flexible, Transparent and Self-Cleanable Superhydrophobic Films Prepared by a Facile and Scalable Nano-pyramid Formation Technique. *Nanoscale* **2014**, *6*, 1453−1461.

DOI: 10.1021/am5086066
ACS Appl. Mater. Interfaces 2015, 7, 5289−5295